THE ASTROPHYSICAL JOURNAL, 314:252–260, 1987 March 1

FOURIER COEFFICIENTS OF VARIABLE STARS. II. LIGHT-CURVE ANALYSIS

R. F. STELLINGWERF AND M. DONOHOE
Mission Research Corporation
Received 1986 August 4; accepted 1986 August 26

ABSTRACT

In Paper I of this series simple models were used to generate a set of radial velocity curves showing the effect of varying amplitude and central condensation of a star. Fourier analysis of these curves produce amplitudes in excellent agreement with observations. A single parameter adequately describes the variation in the shape of all the velocity curves considered: the skewness of the curve.

In this paper, light curves generated by a nonadiabatic nonlinear one-zone model are considered. A set of curves with nearly constant skewness are used to show the importance of a second parameter: the narrowness or "acuteness" of the curve, defined in the same way as the skewness parameter. This property of the light-curve shape is responsible for the smooth variation of Fourier phases seen in RR Lyrae stars and many Cepheids. In the one-zone model, the value of the acuteness is determined by the opacity variation in the deep envelope below the ionization zones, and it could prove to be a probe of interior stellar structure.

Subject headings: stars: Cepheids — stars: pulsation — stars: RR Lyrae — stars: variables

I. INTRODUCTION

This is the second in a series of papers attempting to relate observed characteristics of variable-star light curves to physical parameters of the star. In Paper I (Stellingwerf and Donohoe 1986) a nonlinear, adiabatic one-zone model was used to produce a grid of velocity curves of varying shapes. It was shown that as the amplitude or central condensation of the model is varied the velocity curve changes from sinusoidal to "sawtooth" in shape. The parameter that best describes this change is the "skewness," defined to be the ratio of the duration of the falling branch of the curve to that of the rising branch of the curve, both defined by the sign of the first derivative. It was also shown that the characteristics of observed stars correlate well with skewness.

Fourier parameters were obtained for the models of Paper I and compared with observations. The amplitudes agreed with those of observed stars both in magnitude and in their variation with skewness. The phases agreed with those of particular stars but did not vary as observed. This was shown to be due to the constraint on the phases imposed by the "top-bottom" symmetry of the velocity curves. This symmetry is not present in the light curves. In this paper, the analysis is extended to light curves produced by a nonlinear, nonadiabatic model, and the observed variation of the phases is obtained.

References to recent work in this field may be found in Paper I, in Simon (1986), in Petersen (1984), and in Kovács, Shlosman, and Buchler (1986). Further discussion of the one-zone model, including convection, is given in Stellingwerf (1986). The technique of Fourier analysis of variable-star light curves is of current interest because of the resonance phenomenon found in sequences of Cepheid light curves, and the regular variation of the parameters for RR Lyrae stars. Although some progress has been made in classifying observations using this tool, very little is known about how the derived parameters relate to the constitution of the stars themselves. This work is an attempt to clarify this issue.

II. MODEL DESCRIPTION

Details of the nonadiabatic one zone model are given in Stellingwerf (1972, hereafter S72). This model differs from the adiabatic case discussed in Paper I in several respects.

1. The time scale is one period instead of the dynamic time; this means that some parameters (such as ζ) and the velocity scale are defined differently.

2. The density exponent m is variable. This induces larger nonlinear effects at a given amplitude and is more realistic. It is given by

$$m = \frac{d \log(\rho)}{d \log(r)} = \frac{\log[(r^3 - \eta^3)/(1 - \eta^3)]}{\log(r)}, \qquad (1)$$

where $\eta = r_c/r_0$ is the ratio of the fixed core radius to the total radius.

3. To determine model parameters, the pulsation Q is specified, then η is varied to obtain unit period.

The light curves are obtained by a process of double iteration: first η, the shell thickness, is varied to obtain a period of unity, then the initial value for h, the nonadiabaticity variable, is varied to attain periodicity. This is a device to produce periodic light curves for a model in which the pulsations are growing or dying (the velocity curves so obtained are not periodic). All of these variables and techniques are described in detail in S72.

The effects of the amplitude and shell thickness were explored in Paper I and will not be addressed here, except to note that moderate changes in amplitude produce almost no change in the light-curve shape. Also, it was shown in S72 that variation of the nonadiabaticity parameter, ζ (modeling a change in effective temperature) results in variation of the luminosity phase lag, but no change in the "upper-lower" symmetry of the light curve. A parameter was found, however, that does produce this observed asymmetry: the amplitude of the luminosity variation at the base of the pulsating shell (see Fig. 4 of S72). In equation (14) of S72, we put

$$\frac{L_i}{L_0} = X^{-u} , \tag{2}$$

where X is r/r_0 and u is a parameter to be set. The value of u is estimated in § IV to lie in the range:

$$u = 5 \rightarrow 10 . \tag{3}$$

For now, it is taken as an input quantity, and varied in the range 0–20.

Other parameters defined in S72 are fixed at the values:

$$Q = 0.04, \text{ period} = 1.00,$$
$$\text{max radius} = 1.10, \quad \Gamma_1 = 1.10,$$
$$n = 1, s = 3, \zeta = 1 \tag{4}$$

When a light curve has been obtained, a 10th order least-squares Fourier fit is computed as described in Paper I. In this case the mean Fourier amplitude, m_0, is not equal to the mean magnitude, and the standard phase shift is defined relative to the Fourier mean, not the arithmetic mean of the curve. This is illustrated in Figure 1: the standard phase convention used here is to define a phase of 0.5 to be the phase of m_0 on the rising branch.

III. MODEL RESULTS

Six standard models were computed in the fashion described above, with values of u given by

$$u = 0, 2, 5, 10, 15, 20 . \tag{5}$$

Light curves for the six cases are shown together in Figure 2 and individually in Figure 3. The parameters and results for the six cases are given in Table 1, where m_{eq} is the equilibrium value of the density exponent, given by

$$m_{eq} = \frac{3}{(1 - \eta^3)} , \tag{6}$$

Sk is the skewness, Ac is the acuteness (see below), σ is the standard deviation of the 10th order Fourier fit, Fourier m_0 is the mean luminosity as derived in the Fourier fit, amplitude is the actual measured amplitude of the fit, and the remaining quantities are the Fourier parameters, defined in Paper I. All phases are given on a scale of 0–2π.

Variation of the interior luminosity is shown in Figure 4 for the case $u5$. The amplitude of the interior luminosity variation scales with u, but the phasing is nearly constant. Note the 90° phase lag of the luminosity after the interior luminosity.

Figure 4 also illustrates the definition of the two parameters chosen to describe the shape of the light curve. The parameter discussed in Paper I is the skewness: the ratio of the phase duration of the "descending branch" to that of the "rising branch" (shown in Fig. 4). The other parameter, defined similarly, is the "acuteness": the ratio of the phase duration of lower than average light to that of greater than average light. Note that the mean used here is the average of maximum and minimum brightness. If ϕ_{rb} is the phase duration of the rising branch and ϕ_{fw} is the phase duration of brighter than average light (equal to the full width at half-maximum of the curve), then we have

$$\text{Sk} = \text{skewness} = \frac{1}{\phi_{rb}} - 1 \tag{7}$$

and

$$\text{Ac} = \text{acuteness} = \frac{1}{\phi_{fw}} - 1 . \tag{8}$$

A plot of Sk and Ac versus u is shown in Figure 5. We see that for this sequence of models Ac varies smoothly from less than unity to greater than 4, while Sk remains in the 2–2.5 range. This behavior is consistent with our aim to look only at the effects of Ac on the Fourier parameters while holding Sk fixed. In actual stars, the two quantities are probably highly correlated.

We now turn to the Fourier parameters. Figures 6 and 7 show the trends in the amplitude ratios (the ratio of the amplitude of the nth harmonic to that of the fundamental) as function of Ac. Compare with Figures 4 and 5 of Paper I. We see that the higher harmonic amplitudes increase with Ac, as with

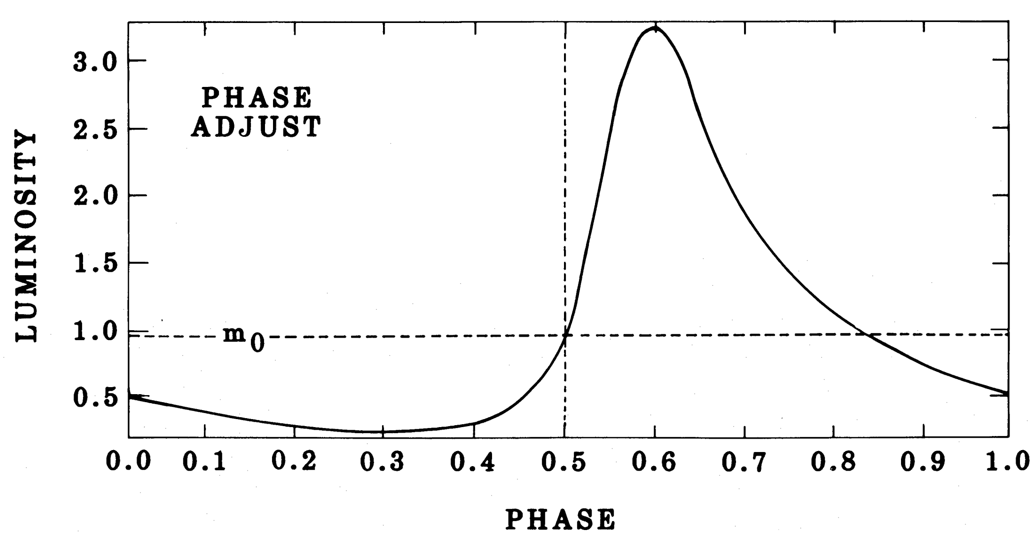

FIG. 1.—Typical computed light curve, showing the chosen phase convention; here m_0 is the Fourier mean amplitude

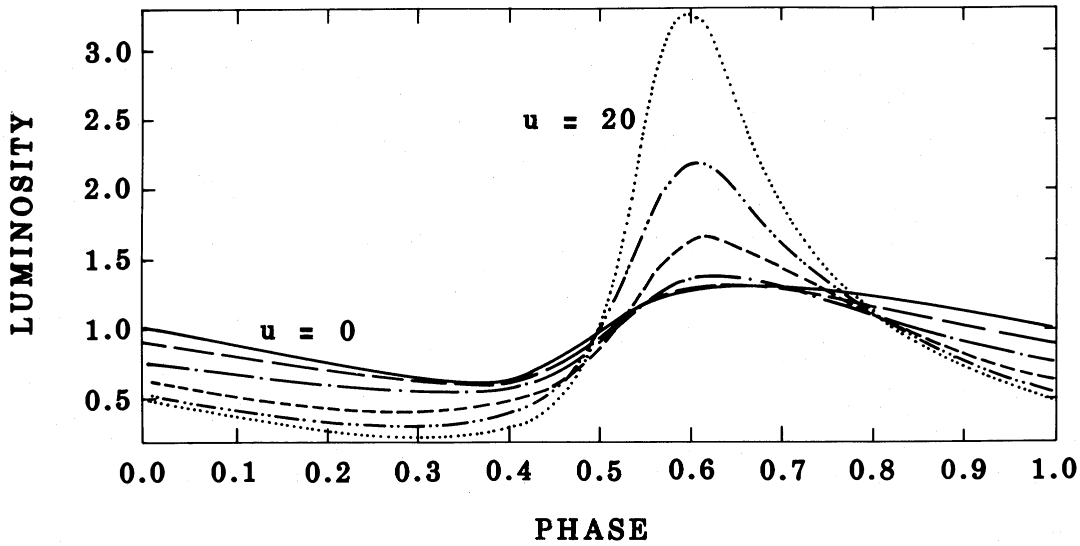

FIG. 2.—Light curves for the six cases described in the text. The $u = 0$ case has the lowest amplitude, the $u = 20$ case has the largest.

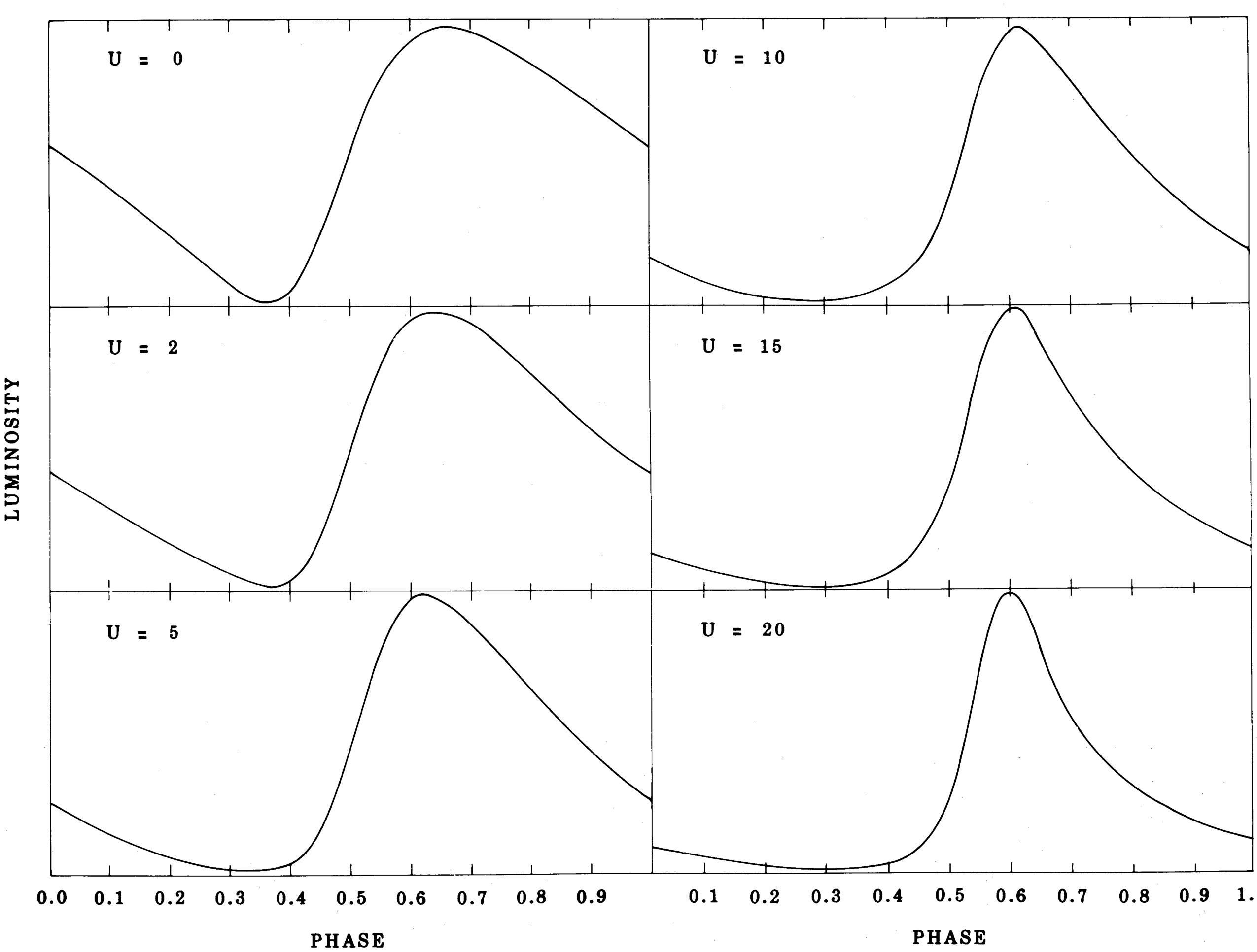

FIG. 3.—Light curves for the six cases, as indicated

TABLE 1

FOURIER FIT PARAMETERS

Model	u0	u2	u5	u10	u15	u20
u	0.000	2.000	5.000	10.000	15.000	20.000
Density $\mathfrak{m}_{eq}$	11.820	11.590	11.270	10.830	10.510	10.170
Sk	2.333	2.704	2.571	1.941	2.125	2.448
Ac	0.818	1.273	1.778	2.448	3.167	4.263
Sigma	0.001	0.001	0.001	0.003	0.004	0.012
Fourier $\mathfrak{m}_0$	0.991	0.935	0.874	0.829	0.861	0.973
Amplitude	0.703	0.724	0.841	1.241	1.886	3.039
H1	0.309	0.320	0.377	0.522	0.725	1.017
R21	0.335	0.356	0.358	0.386	0.463	0.564
R31	0.117	0.135	0.149	0.176	0.237	0.337
R41	0.044	0.054	0.066	0.088	0.127	0.205
R51	0.017	0.022	0.029	0.045	0.069	0.123
R61	0.006	0.007	0.011	0.022	0.037	0.073
R71	0.001	0.001	0.003	0.009	0.018	0.041
R81	0.001	0.002	0.002	0.004	0.007	0.020
R91	0.002	0.002	0.003	0.003	0.002	0.009
R101	0.002	0.002	0.003	0.004	0.003	0.005
PHI1	1.501	1.663	1.848	1.946	2.059	2.135
PHI2	4.732	4.595	4.557	4.550	4.704	4.773
PHI3	1.852	1.503	1.233	0.993	1.130	1.175
PHI4	5.336	4.779	4.279	3.764	3.847	3.862
PHI5	2.538	1.747	1.024	0.245	0.267	0.253
PHI6	5.832	4.872	3.935	2.957	2.950	2.908
PHI7	2.021	0.953	0.102	5.519	5.600	5.556
PHI8	3.688	2.437	1.542	1.348	1.878	1.910
PHI9	0.199	5.110	3.909	3.075	4.139	4.436
PHI10	3.041	1.521	0.124	4.942	3.977	2.247
PHI21	1.729	1.270	0.862	0.658	0.586	0.504
PHI31	3.631	2.798	1.973	1.438	1.237	1.054
PHI41	5.615	4.412	3.171	2.264	1.896	1.607
PHI51	1.315	6.000	4.351	3.082	2.540	2.146
PHI61	3.108	1.179	5.415	3.849	3.165	2.666
PHI71	4.079	1.880	6.017	4.465	3.756	3.180
PHI81	4.245	1.702	5.609	4.631	4.259	3.683
PHI91	5.539	2.713	6.128	4.412	4.462	4.074
PHI101	0.596	3.743	0.496	4.333	2.241	6.033

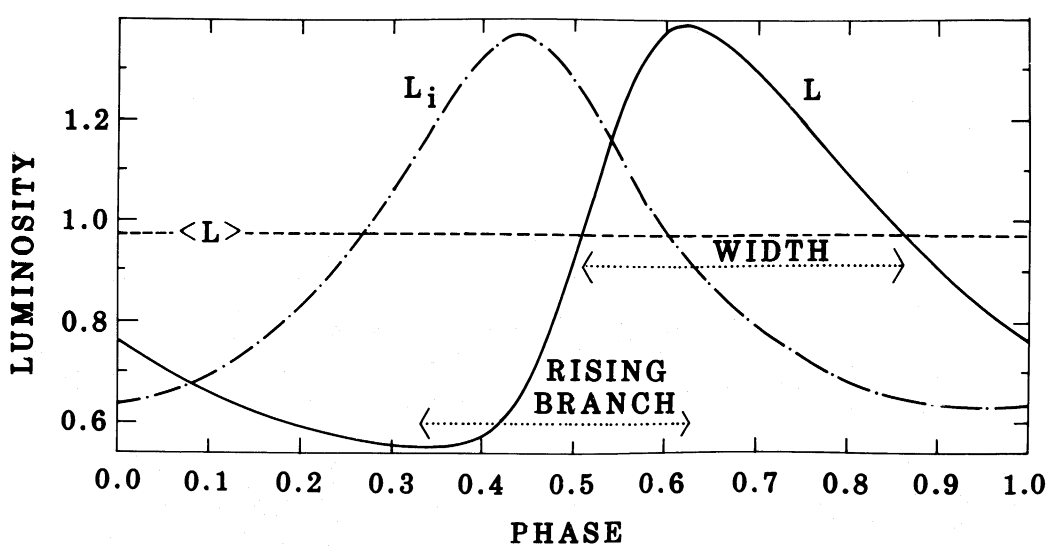

FIG. 4.—Variation of the interior luminosity (*dashed line*) and the exterior luminosity of model $u = 5$. Also shown are the two phase ranges used to define the skewness and the acuteness (*see text*).

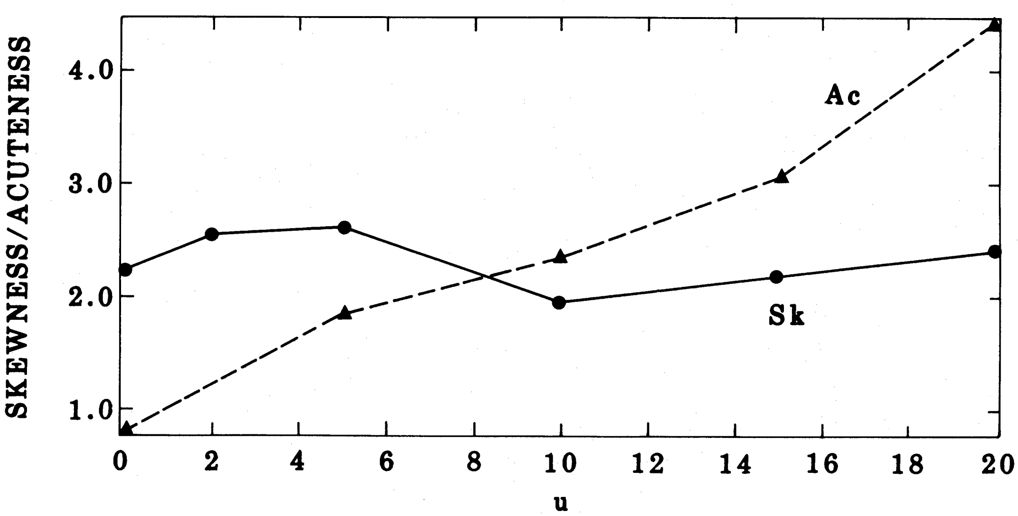

FIG. 5.—Variation of the skewness (Sk) and the acuteness (Ac) as functions of the parameter *u*

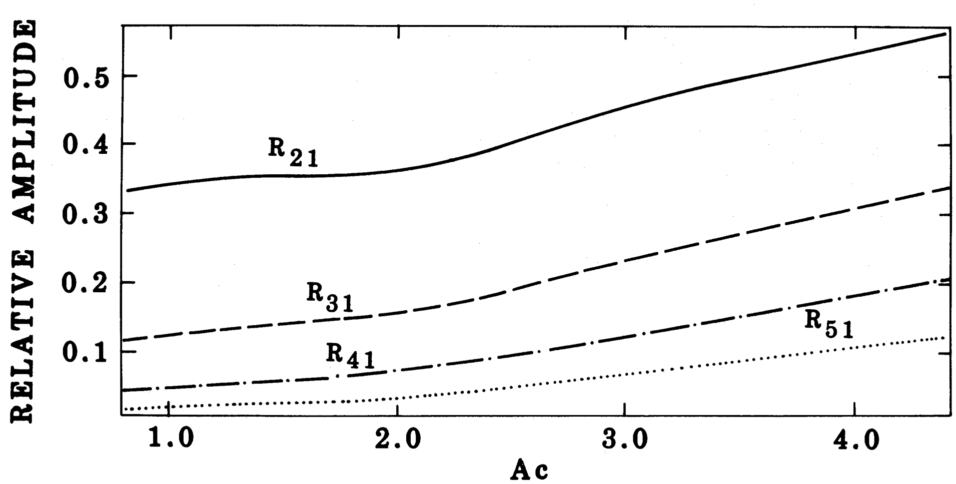

FIG. 6.—Variation of the low-order relative Fourier amplitudes vs. Ac

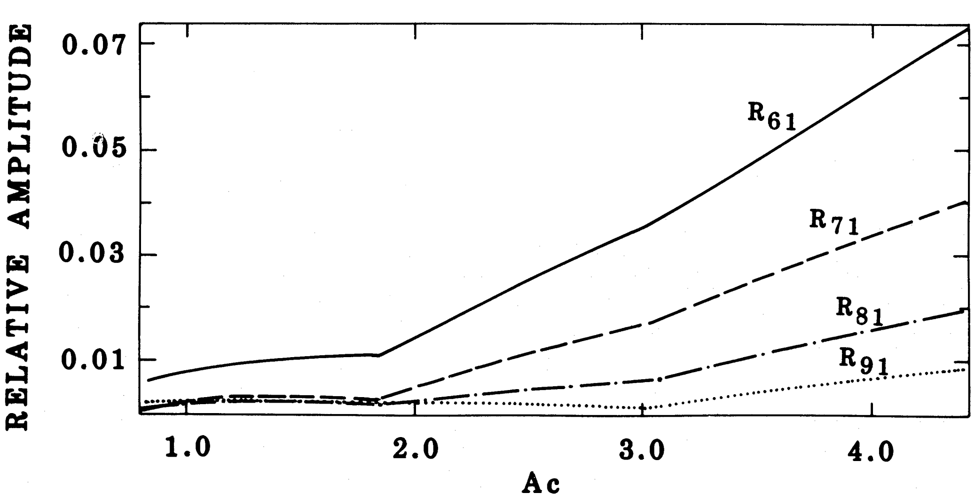

FIG. 7.—Variation of the high-order relative Fourier amplitudes vs. Ac

Sk, but do not go to zero at unity as in the velocity curves of Paper I, or increase as rapidly, at least for the first few harmonics. The conclusion is that the amplitudes of harmonics 2–5 are determined primarily by Sk, while those of harmonics 6–9 are influenced both by Sk and Ac. Amplitudes of RR Lyraes in ω Cen are given by Petersen (1984) and are in agreement with the model amplitudes shown here, for skewness = 2–3.

For the low u models, the values obtained for ϕ_1 in Table 1 are near $\pi/2$, and those of ϕ_2 are near $3\pi/2$, both in agreement with the values obtained for the velocity curves in Paper I. In Paper I, a clear, predictable pattern was found for the higher harmonics: the ϕ_N values relaxed to a constant value at a harmonic level determined by the skewness. This pattern is not present in the current models. If anything, the ϕ_{N1} values seem to settle down to a pattern that could be a nearly constant value, a slow increase, or a set of grouped values. This is caused by the complicated shape of the light curves and occurs at lower harmonics for higher Ac values.

IV. COMPARISON WITH OBSERVATIONS

In Paper I we noted that the Fourier phases of the adiabatic models show only abrupt jumps as a function of Sk. Observations of both Cepheids and RR Lyrae stars, however, show a smooth and distinctive variation of the phases as a function of period or skewness. We hypothesize that the observed variation is caused by changes in Ac. Plots of the phase differences versus Ac for the models are shown in Figures 8 and 9. A rather strong and smooth variation is seen for all harmonics. For comparison, Figure 10 shows a portion of Figure 8b of Paper I: Petersen's data for ω Cen (1984), where the mean lines have been drawn in by eye, and the scale is the same as Figure 9. The agreement between Figure 10 and Figure 9 in the range Ac = 1–2.5 is almost exact. Although Ac measures for Petersen's stars are not available, the prediction based on the present analysis is, for ω Cen:
for average stars in the range:

$$\mathrm{Sk} = 1 \rightarrow 6\ ;$$

we predict:

$$\mathrm{Ac} = 1 \rightarrow 2.5\ . \tag{9}$$

Such a variation of Ac, if verified, would totally account for the phase variations observed.

Another sensitive diagnostic of the Fourier phases is the "phase-phase" plot, discussed by Simon and Moffett (1985) and shown as Figures 12 and 13 of Paper I. These figures are

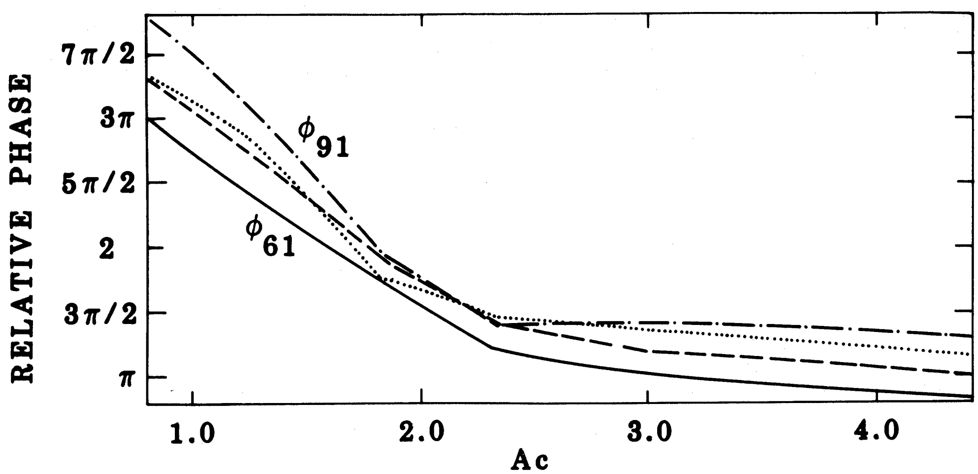

FIG. 8.—Variation of the low-order relative Fourier phases vs. Ac

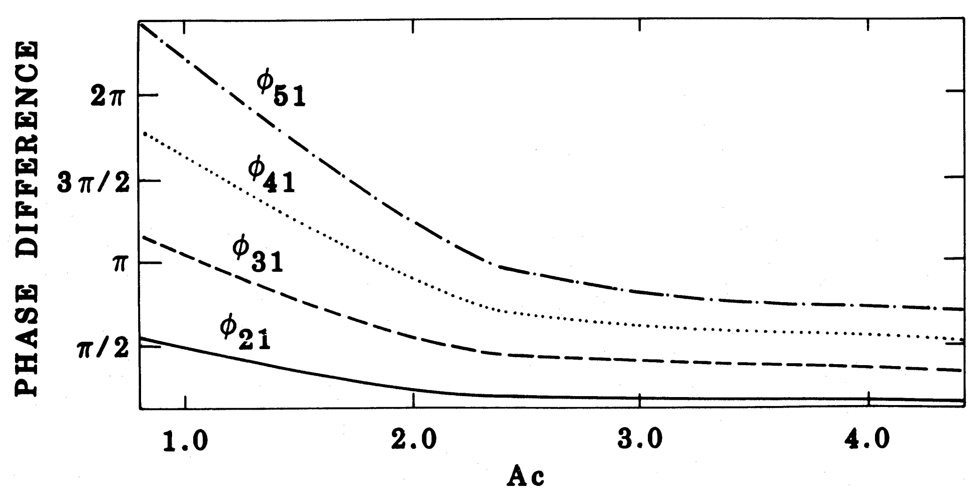

FIG. 9.—Variation of the high-order relative Fourier phases vs. Ac

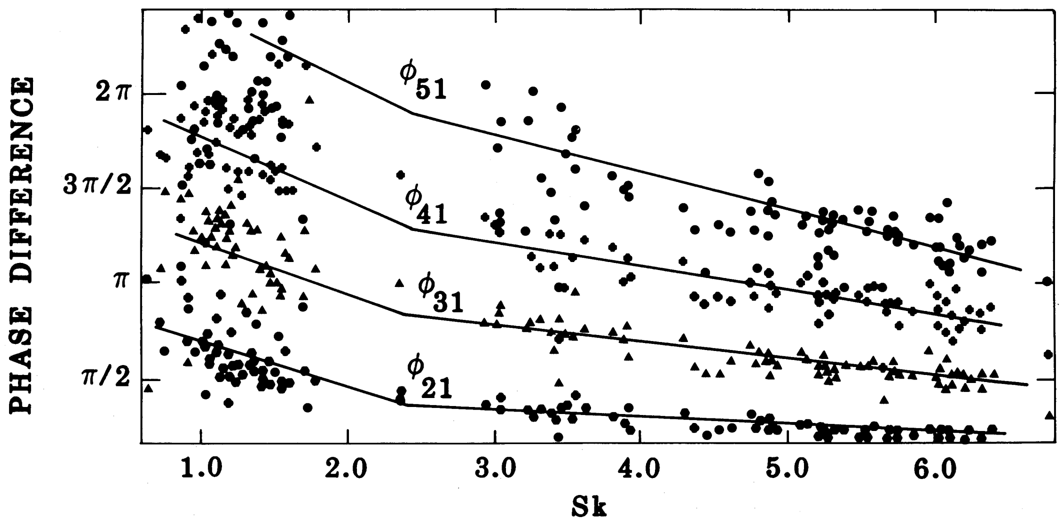

FIG. 10.—Variation of the low-order relative Fourier phases vs. Sk for observed RR Lyrae stars: Petersen (1984) data for ω Cen

reproduced here as Figure 11, showing the ϕ_{21}/ϕ_{31} plane, and Figure 12, showing the ϕ_{31}/ϕ_{41} plane. The models of Paper I are indicated by the open circles, and the generalization to a constant phase shift is indicated by the dashed line labeled "adiabatic." The Cepheids analyzed by Simon and Moffett (1985) are plotted as filled triangles and the ω Cen data of Petersen (1984) is represented by the shaded mean lines. The present models are plotted as a solid line. We see that the models represent the RR Lyrae data very well and also follow the Cepheid data much better than the adiabatic trend line. Two features in the Cepheid data are not reflected in the models: the lack of ϕ_{21} values in the range $0 \rightarrow \pi/2$ and the apparent parallel sequence of stars with ϕ_{41} displaced downward by $\sim\pi/2$. These features are quite likely associated with the resonance expected at a period of ~ 10 days.

We conclude that these models represent the Fourier parameters of actual stars remarkably well, especially those of RR Lyrae stars.

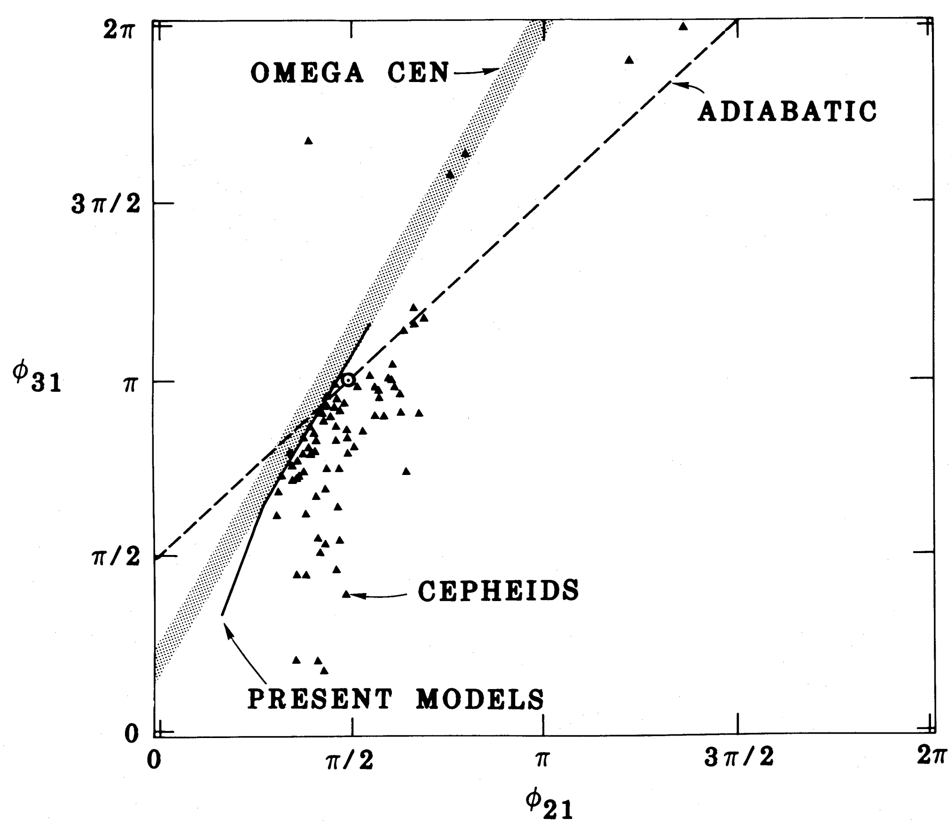

FIG. 11.—Phase-phase plot showing the locus of models and observed stars on the ϕ_{21}/ϕ_{31} plane. *Solid line*: present models; *dashed line*: adiabatic models; *shaded line*: RR Lyrae stars in ω Cen (*median line*); *filled triangles*: Cepheids; *open circle*: models of Paper I.

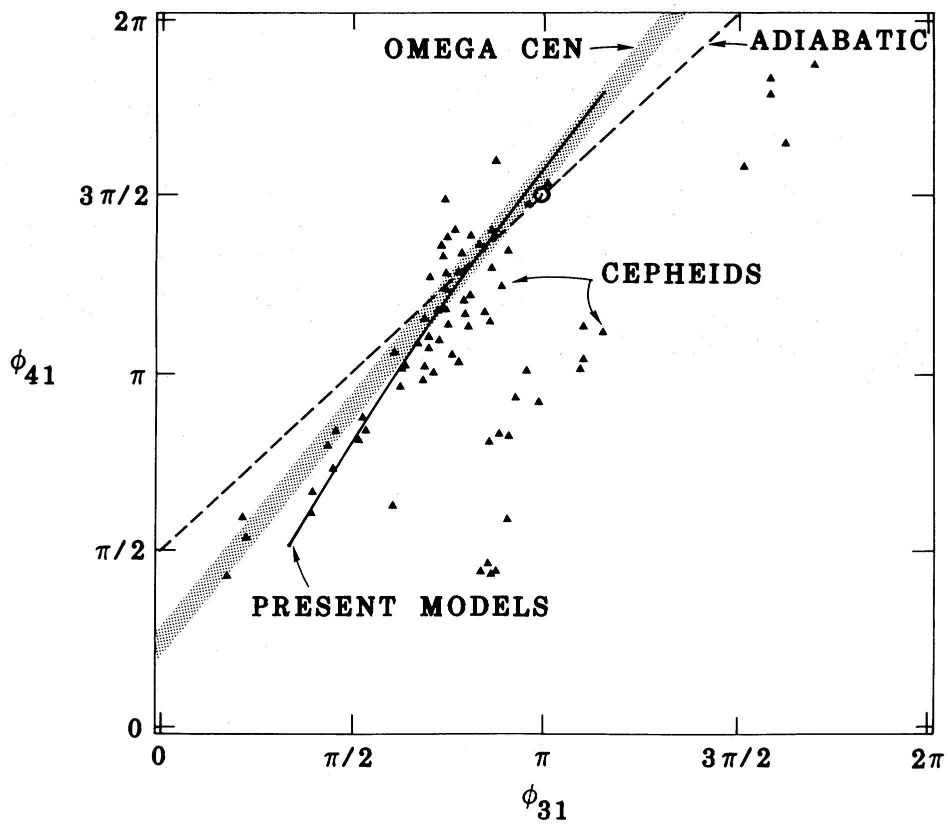

FIG. 12.—Same as Fig. 11 but for the ϕ_{31}/ϕ_{41} plane

V. INTERPRETATION

We have identified two primary characteristics of light and velocity curves that affect the Fourier parameters: the skewness, Sk, and the acuteness, Ac. For the first few harmonics, the Fourier amplitudes depend primarily on Sk, while the phases depend on Ac.

Looking at the model, we find that Sk and Ac are determined by very different physics. Sk is a measure of the mechanical nonlinearity of the envelope pulsation. For the simple models, the skewness depends only on the amplitude of the velocity curve, with a very weak dependence on the thickness of the pulsating shell.

Ac, on the other hand is primarily a light-curve parameter and its determined by the thermal properties of the star. In the model it is a function of the amplitude of the light variation at the base of the driving regions of the envelope of the star. This variation is caused by temperature variation in the relatively deep, nearly adiabatic regions below the ionization zones that contribute the bulk of the radiative damping of the pulsation. Ac measures the ratio of the light to the radius variation in these deep layers. By equation (13) of Paper I, we have

$$u = m[(s + 4)(\Gamma_1 - 1) - n] - 4 , \qquad (10)$$

where the values of m, s, n, and Γ_1 refer to the interior, not the shell. Here m has the value 3 or a bit larger, n and s are the density and temperature exponents of the opacity and have the values 1 and 0–3, and Γ_1 is 5/3. We can thus make a table of u as a function of s (*see* Table 2). Consulting Figure 5, we see that this range of u ($1 \rightarrow 9$) implies a range of Ac of $1 \rightarrow 2.2$. From equation (6), we see that this is exactly the range of u obtained from comparison with the ω Cen observations. The implication here is that at differing effective temperatures in the instability strip, the effective value of s changes over its maximum range, probably reflecting the changing depth of the ionization regions.

TABLE 2

ESTIMATED VALUES OF u AS A FUNCTION OF s

s	$u\,(m = 3)$	$u\,(m = 3.5)$
0	1	1.83
1	3	4.17
2	5	6.50
3	7	8.83

One caveat is in order here. It is known that details of the light-curve shape can be influenced by shock-wave development in the vicinity of the hydrogen zone (Castor 1968). We expect that such processes will modify the results obtained here, especially for large-amplitude pulsators. The detailed agreement of the present results with observation is strong evidence, however, that a very simple model suffices to explain the bulk of the observational data.

Another point is the lack in these models of the abnormalities in Fourier phases seen in Cepheids with periods near 10 days (Simon and Lee 1981). This is consistent with the explanation of the Cepheid behavior as a resonance phenomenon, since no resonance is possible in a one-zone model.

The authors would like to thank J. O. Petersen for the use of his ω Cen data, and, along with N. R. Simon, for valuable discussions. This research is supported by National Science Foundation grant AST84-11029, through Mission Research Corporation.

REFERENCES

Benz, W., and Mayor, M. 1982, *Astr. Ap.*, **111**, 224.
Castor, J. I. 1968, *Ap. J.*, **154**, 793.
Kovacs, G., Shlosman, I., and Buchler, J. R. 1986, *Ap. J.*, **307**, 593.
Petersen, J. O. 1984, *Astr. Ap.*, **139**, 496.
Simon, N. R. 1986, *Ap. J.*, **311**, 305.
Simon, N. R., and Lee, A. S. 1981, *Ap. J.*, **248**, 291.
Simon, N. R., and Moffett, T. J. 1985, *Pub. A.S.P.*, **97**, 1078.
Stellingwerf, R. F. 1972, *Astr. Ap.*, **21**, 91 (S72).
———. 1984, *Ap. J.*, **284**, 712.
———. 1986, *Ap. J.*, **303**, 119.
Stellingwerf, R. F., and Donohoe, M. 1986, *Ap. J.*, **306**, 183 (Paper I).

Mary Donohoe and Robert F. Stellingwerf: Mission Research Corporation, 1720 Randolph Road, SE, Albuquerque, NM 87106